FUSION PRODUCT DIAGNOSTICS OF TOKAMAK PLASMAS

Vasily Kiptily

Culham Centre for Fusion Energy
EURATOM Association, Culham Science Centre, Abingdon, OX14 3DB United Kingdom
vasili.kiptily@ccfe.ac.uk

ABSTRACT

This lecture reviews the fusion product diagnostics that are currently used for study of tokamak plasmas. Neutrons and charged fusion product measurement techniques as well as γ-ray diagnostics will be described together with examples obtained in experiments on JET (UK). Developments for ITER are discussed. The detailed information on the issues of the lecture can be finding in the reviews [1-3].

I. INTRODUCTION

Fusion product diagnostics can be used to determine a fusion reaction rate, which indicates how close the plasma is to the ultimate goal of making a power plant based on nuclear fusion. However, these diagnostics can also provide large amounts of additional information, such as ion temperatures, the thermonuclear fraction in the fusion reaction rate, degree of fast-ion confinement, fast-ion loss mechanism, etc.

Each section of this lecture contains a general explanation of these systems, showing some experimental results obtained on working machines. A lot of useful information on the behaviour of energetic particles and their degree of confinement is provided in present D-D experiments since non-thermal ions contribute dominantly to the fusion reaction rate. Here are D-D reactions

$$D + D \rightarrow t(1.0MeV) + p(3.0MeV)$$

and

$$D + D \rightarrow {}^3He(0.8MeV) + n(2.5MeV)$$

have been the primary diagnostic tools. The D-^{3}He reaction

$$D + {}^3He \rightarrow {}^4He(3.7MeV) + p(14.7MeV)$$

has been used for diagnosing the plasma when ^{3}He is introduced for the discharge.

In future D-T experiments on ITER, the contribution of the fusion reaction

$$D + T \rightarrow {}^4He(3.5MeV) + n(14.1MeV)$$

will be increased and the combination of several neutron measurement systems will provide the absolute fusion output and neutron fluence on the first wall. Cross-sections of the fusion reactions are well known (see Fig.1) and can simply be calculated using parameters from [4].

Together with neutron measurement, NPA, γ-ray and the fast-ion/α-particle loss measurements play important roles in research on burning plasma physics and hence in the self-heating burning control of the device.

II. NEUTRON DIAGNOSTICS

This chapter is dedicated to measurements of the neutron emission rate, neutron emission profiles and energy spectra. There have been several review articles on neutron diagnostics, and Ref.5 is recommended for the neutron diagnostics details.

II.A. Neutron emission rate measurements

The absolute measurement of neutron emission rate from the whole plasma is a very important diagnostic as a fusion power monitor in fusion experiments with D-D or D-T plasmas. So, the neutron emission rate will be used as a feedback parameter for fusion output control in ITER or other burning plasma devices.

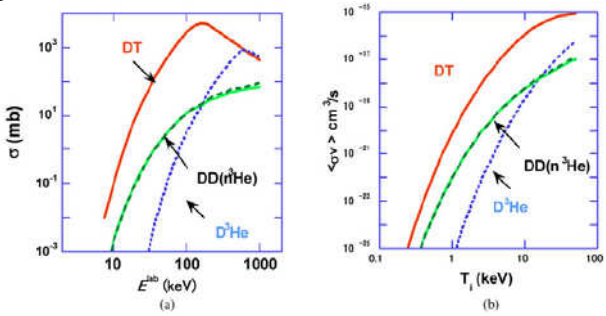

Fig.1. Fusion cross sections (a) as a function of the CM energy of the reacting particles and fusion reactivities (b) for Maxwellian ion distributions as a function of ion temperature *Ti*.

In fusion experiments with auxiliary heating, such as NBI, the neutron emission rate changes from 10^4–10^6 over the time scale of the fast ion slowing-down time (~100 ms). Therefore, the detector of the neutron emission rate must have a wide dynamic range and fast response time and also be immune to spurious signals from hard X-rays and γ-rays. To implement these two requirements simultaneously, a fast response neutron detector that selectively produces a large signal only for neutrons is used in combination of two operation modes: a pulse-counting mode and the current mode. The BF_3 proportional counters, ^{3}He proportional counters, and ^{235}U fission chambers are the most commonly used neutron detectors [6]. The BF_3 and ^{3}He proportional counters utilize $^{10}B(n,\alpha)^7Li$+2.78 MeV and $^3He(n,p)T$+0.77 MeV reactions, respectively. The ^{235}U fission chambers utilize the

^{235}U(n,fission) reaction producing ~ 200 MeV of energy. As the energy dependence of these reactions is proportional to $E^{-1/2}$, these detectors are more sensitive to low-energy neutrons. To detect higher-energy neutrons, these detectors are often used with moderators to slow down fast neutrons. A fission chamber is an ionization chamber with electrodes coated with fissile material such $^{\text{as } 235}$U or ^{238}U, and ionization of the chamber gas is caused by fission fragments produced at the electrode with kinetic energy of 50 to 200 MeV. Here, it should be noted that ^{238}U fission chambers are sensitive only to fast neutrons because the ^{238}U(n,fission) reaction has a threshold of ~1 MeV.

The neutron activation system provides time-integrated measurements of the total neutron yield with high degree of accuracy using well-known neutron reaction cross-sections. If the irradiation point is installed near the plasma, the relation between the neutron emission rate in the whole plasma and the neutron flux at the irradiation point should be calibrated by neutron Monte Carlo calculation with precise machine modelling.

The primary goals of the neutron activation system are to maintain a robust relative measure of fusion energy production with stability and a wide dynamic range, to enable accurate absolute calibration of fusion power. Fluxes of D-D and D-T neutrons can be measured easily with several foils with different threshold energy reactions. From the ratio of D-D and D-T neutron fluxes, the triton burn-up ratio in D-D plasmas and the D/T fuel ratio (n_d /n_t) in D-T plasmas can be derived. A sophisticated multi-foil activation technique using an unfolding code can provide a neutron energy spectrum at the irradiation point which is useful for testing of the neutron transport calculations.

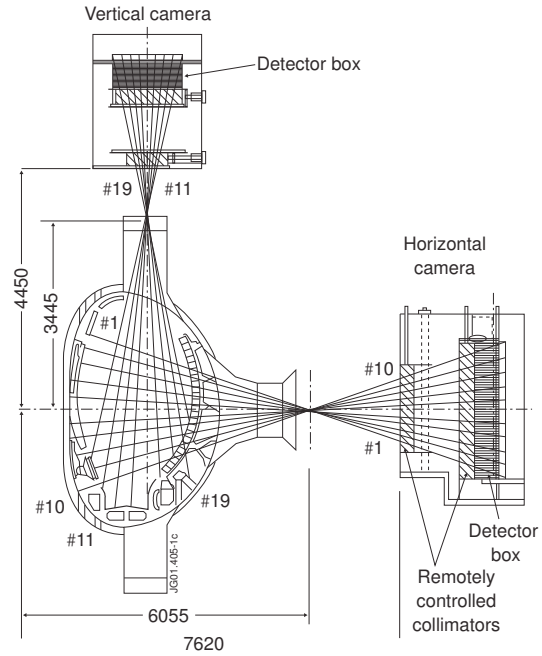

Fig.2 Schematic view of JET neutron profile monitor.

The neutron activation method using solid samples is used for accurate measurement of the neutron yield in many fusion devices. At current large tokamaks, pneumatic operated sample transfer systems are employed using polyethylene capsules. JET has multiple irradiation positions with different poloidal locations, while JT-60U has a single position of the irradiation end in a horizontal port. A capsule with sample foils can be transferred to the selected irradiation end via a "carousel" switching system from a capsule loader in the γ-ray counting station before a plasma shot. After the plasma shot, each capsule returns to the γ-ray counting station by the pneumatic transfer system. Gamma-rays from the activated samples are measured with HPGe or NaI(Tl) scintillation detectors. In the case of fissile samples, such as ^{232}Th or ^{238}U, delayed neutrons from the irradiated samples are measured with high-sensitivity neutron detectors, such as ^{3}He or BF_3 proportional counters.

II.B. Neutron emission profile systems

The neutron source in fusion plasmas consists of a thermonuclear component and a component produced by fast fuel ions (deuterons, tritons). The thermonuclear neutron source profile is usually a function of the magnetic surfaces, but this is not true for the neutron source component related to fast ions. Their behaviour in reactor plasmas is crucially important, especially in driven regimes approaching the ignition. Measurements of spatial and energy distributions of fast confined fuel ions are very important for optimization of NBI and ICRF heating and current drives.

Neutron source profile measurement is the principal method for the measurement of fast fuel ion distributions. Because of non-symmetric deposition of NBI and ICRF-driven ion distributions on magnetic surfaces, the two-dimensional (2-D) neutron source profile measurements are required. This requirement is becoming stronger for optimization of ignition in reactors and plasmas influenced by magneto-hydrodynamic (MHD) instabilities.

The primary function of a neutron profile monitor is to measure the neutron emissivity over a poloidal cross section of the plasma using line-integrated measurements recorded by neutron detectors viewing the plasma along a number of chords (lines of sight). Knowledge of the absolute detection efficiency of the system enables us to obtain the total instantaneous neutron yield from the tokamak independently supplementing the results obtained using other techniques, such as neutron activation or neutron flux monitors.

The JET neutron profile monitor is a unique instrument among diagnostic systems available at large fusion devices. The solution adopted in JET for imaging of the noncircular plasma neutron source is to use two fan-like multi-collimator detector arrays as illustrated in Fig.2 A nine-channel camera is positioned above the vertical port to view downward through the plasma (vertical camera), while a ten-channel assembly views horizontally from the side (horizontal camera). The collimation can be remotely adjusted by use of two pairs of rotatable steel cylinders. Each channel is equipped with a set of three different detectors: a NE213 liquid organic scintillator with pulse shape discrimination (PSD) electronics for simultaneous measurement of 2.5 MeV D-D neutrons, 14-MeV D-T neutrons, and γ-rays; a BC418 (Bicron) plastic scintillation detector for measurement of 14-MeV D-T neutrons; and a CsI(Tl) photodiode for measuring the fast-electron bremsstrahlung and γ-ray emission in the range between 0.2 and 6 MeV. Each NE213 detector-photomultiplier unit is equipped with two PSD units allowing neutrons to be separated from γ-rays and providing the necessary energy discrimination. The Bicron scintillators are located in front of

the NE213 scintillators and are coupled to PMTs via a light guide. They are sufficiently small and therefore relatively

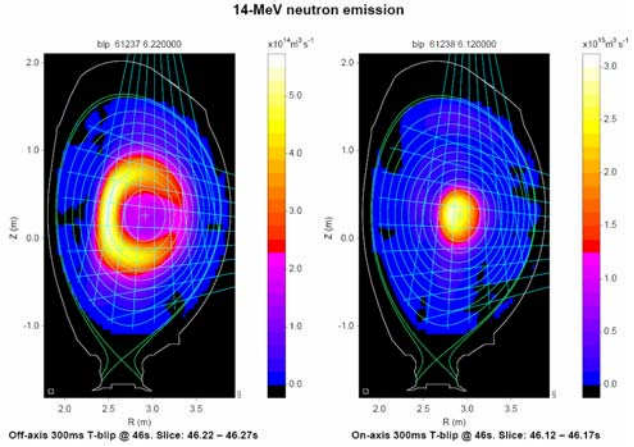

Fig.3 Tomographic reconstruction of data obtained with JET neutron cameras in TTE: left – off-axis tritium NBI blip; right – on axis one.

insensitive to γ-rays with $E_\gamma > 2$ MeV. The detection efficiencies for each of the 19 channels (and for both D-D and D-T neutrons) are determined computationally and by taking into account accelerator-based absolute calibrations of the scintillation detectors. The JET also complements activation systems and neutron flux monitors, providing an independent estimate of the absolute neutron yield from the plasma.

The JET profile monitor allows 2-D images to be obtained from the plasma neutron emission. Tomographic deconvolution of the line-integrated measurements is carried out with TOMO5 code [7] to obtain a 2-D mapping of the neutron emission rate. The plasma coverage by neutron profile arrays is adequate for neutron tomography, although neighbouring channels are 15 to 20 cm apart and have a width of ~ 7 cm as they pass near the plasma centre.

Capabilities of this method are illustrated in Fig.3 or two

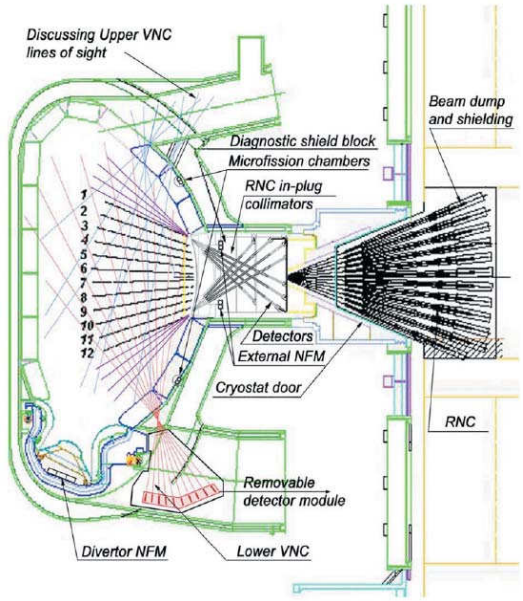

Fig. 4. Arrangement of the 2-D neutron source strength and energy distribution measurements in ITER.

JET discharges with injection of tritium beam into D-D plasmas in the Trace Tritium Experiments (TTE). These discharges were characterized by the off-axis and on-axis injections into L-mode monotonic current profile plasmas. In the off-axis injection case, a banana-shape 14-MeV neutron emission is on the high-field site. The on-axis beam-injection generates neutron emission in the plasma centre.

The necessity of 2-D neutron profile measurements in ITER arises from the fact that, due to fast ion components, the neutron source profile will not be constant on magnetic surfaces, especially during ICRH, NBI, sawtooth oscillations, excitation of Alfven eigenmodes, and in advanced tokamak regimes with strongly negative magnetic shear. The 2-D neutron source strength and energy distribution measurements in ITER could be made by joint application of radial neutron camera (RNC) including compact in-plug collimators and vertical neutron cameras (VNC) showed in Fig.4. The RNC consists of 12x3 fan-shaped arrays of collimators viewing the plasma through a special shielding plug in equatorial port #1 and additional channels placed inside this equatorial port.

Several possible arrangements of the VNC have been studied, including distributed and upper VNC. The main concept of the lower VNC arrangement is to place the VNC shielding module inside a divertor port with collimators viewing the plasma through the gaps in the divertor cassettes, the blanket

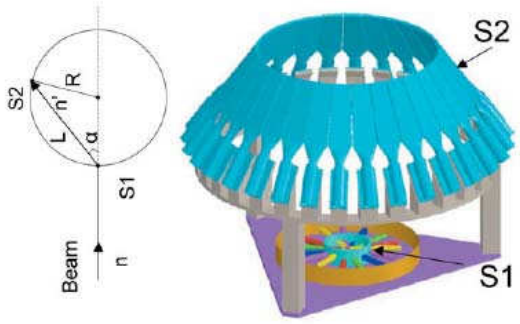

Fig. 5. Scheme of TOFOR spectrometer.

modules, and the triangular support.

II.C. Neutron spectrometry

The neutron emission spectrometry is a multi-function diagnostic the information of which is derived from measurement of the energy distribution of the direct and scattered neutron flux from plasmas.

The spectrum of direct plasma neutron emission reflects the relative motions of the fuel ions given by their velocity distributions. The neutron emission varies in both intensity and spectrum shape as the plasma heating conditions are changed. With ohmic heating, the ions are in thermal equilibrium and the spectrum shape will be almost precisely Gaussian and the effective ion temperature, Ti, can be deduced simply from the fwhm of the measured spectrum, fwhm = $82.5(T_i)^{1/2}$ for d-d plasmas and $178(T_i)^{1/2}$ for d-t plasmas (keV units). Intensity of neutron emission depends on the fusion reaction rate $R \propto n_1 n_2 \langle\sigma v\rangle_{Ti}$, where n_1, n_2, are the local ion densities and $\langle\sigma v\rangle_{Ti}$ is a fusion reactivity. This temperature is actually an average along the line-of-sight through the plasma. However, since the neutron emission is strongly localized near the plasma centre, the line-

averaged temperature is typically only about 10% lower than the central temperature. The thermal neutron emission is isotropic and has a characteristic peak energy, $E_0(T_i)$. Neutron emission spectra with auxiliary heating (NBI, ICRH) of plasmas have a non-Gaussian shape. Furthermore, rotation of the plasmas relative to a detector leads to the peak energy shift due to the fusion reaction kinematics.

At present JET is the tokamak best equipped for neutron diagnosing with high-performance spectrometers installed. One of them, spectrometer TOFOR is dedicated to measuring 2.5-MeV D-D neutrons in DD plasmas and can reach count rates in the 100-kHz range [8]. It is placed in the roof lab looking vertically down on the plasma at a distance of ~20 m with the sight line perpendicular through the plasma core.

Principles of the TOF spectrometer are shown on Fig.5: an incoming neutron being scattered from a proton in scintillator S1 to scintillator S2 with both detectors placed on the constant TOF sphere. The lower panel shows a model of the TOF spectrometer designed for optimized rate (TOFOR); the height is ~1 m [8].

There is also an upgrade version of the MPR spectrometer (MPRu) for measurement of the entire fusion neutron spectrum in the energy range ≈1.5 to 18 MeV. The incoming neutrons produce proton recoils in the polyethylene target foil. The forward-going protons are focused, analyzed in the pole gap of D1 and D2 magnet and counted in the detector array at the focal plane exit (Fig.6). This is a high-performance instrument for diagnosis of D-T plasmas with count rates in the megahertz range [9]. For D plasmas, it is complementary to TOFOR.

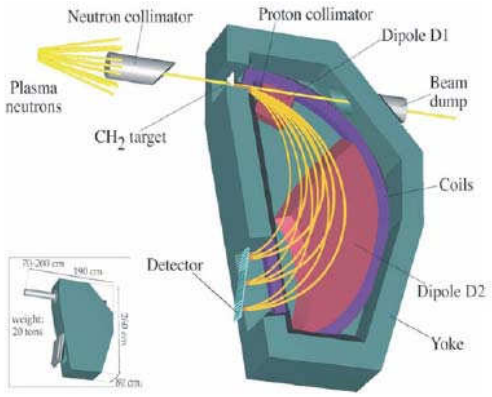

Fig. 6. Scheme of the magnetic proton recoil spectrometer (MPR)

A flux of neutral hydrogen (D, T) atoms is produced in the plasma by three processes: (a CX with background neutrals, (b) radiative recombination of protons (deuterons, tritons) and electrons, and (c) electron capture from hydrogen-like impurity ions. The ratio between these three processes varies depending on particle energy and position in the plasma. The first two processes are dominant in the thermal energy range below 100 to 200 keV, with recombination dominating in the central part of the plasma in large tokamaks. The last process is prevalent in the suprathermal energy range above 100-200 keV. According to this, the thermal energy range is used to study the bulk plasma ion component, whereas the suprathermal range is suitable for the study of high energy ions generated by auxiliary heating like ICRH or produced by fusion reactions in the plasma.

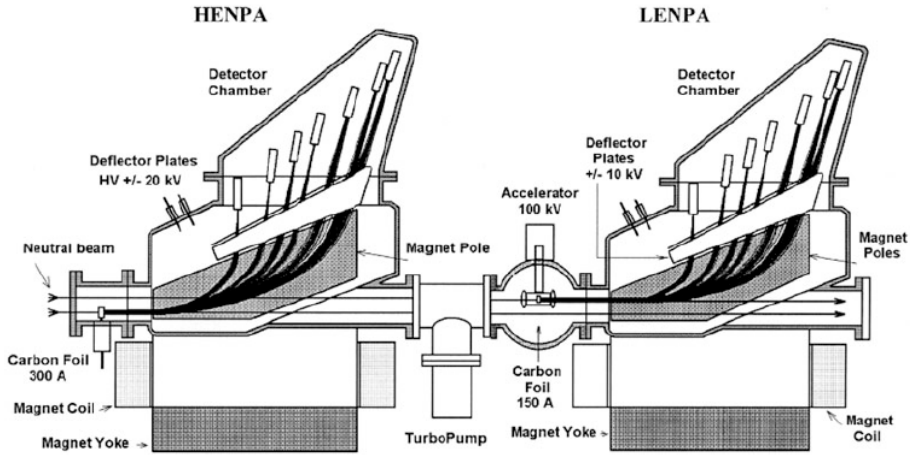

Fig. 7. Layout of NPA diagnostic set up proposed for ITER [12].

III. NEUTRAL PARTICLE ANALYSERS [2]

The charge exchange (CX) neutral particle analysis provides straightforward information concerning parameters of the plasma ion component. The energy spectra of neutral atomic fluxes emitted by the plasma provide not only the ion temperature but also the ion energy distribution function. The latter is important both for understanding the particle and energy confinement mechanisms of the ion component and for studying the behaviour of ions produced by neutral beam heating and by application of ICRF heating.

In the suprathermal range, the neutral flux is produced mainly by H^+, D^+, T^+ ions undergoing electron capture from hydrogen-like low-Z impurity ions. In the case of He^{2+} ions, neutralization in the MeV range occurs by double electron capture from helium-like low-Z impurity ions. The most probable donors for electron capture in large plasma machines like JET are helium-like carbon and beryllium ions because carbon and beryllium are the main low-Z impurities in these machines and their densities in the plasma core are higher than the density of H^0. At energies E>100 keV, the hydrogen-like

ions Be^{3+} and C^{5+} are rather effective donors for neutralization of H^+ in comparison with the residual H^0 atoms.

Neutralization of confined alphas on impurities in D-T plasma creates the possibility to detect the energy spectrum of the fast He^0 atoms and to derive the confined α-particle distribution function. The first successful attempt to do this was made on JET [10]. Another option to measure the flux of suprathermal atoms is to use the pellet CX technique. These measurements obtained with the use of lithium (or boron) pellets injected into the plasma were used in TFTR for measuring the distributions of ICRF-driven H^+-ions and fusion alpha particles [11]. For lithium pellets, H^+ and He^{2+} ions interacted with the pellet ablation cloud of Li^+ to form an equilibrium neutral fraction as a result of the reactions $H^+ + Li^+ \rightarrow H^0 + Li^{2+}$ and $^4H^{2+} + Li^+ \rightarrow {}^4He^0 + Li^{3+}$.

Neutral particle analyzers (NPA) have the following general features. The neutral particle flux from a plasma enters the analyzer and is partially ionized by stripping collisions with molecules in a gas-filled stripping cell or by passing through a thin foil (e.g., a 5- to 40-nm thick carbon foil). The resulting secondary ions are separated by mass and by energy with superimposed or adjacent (tandem-type) electric and magnetic fields or by time-of-flight (TOF) analysis. Then they are detected by a set of ion detectors. Scintillation counters, channeltrons, or microchannel plates MCPs) combined in chevron-type units can be used as ion detectors. Sets of detectors (from 5 up to 40 per mass species) are normally used in NPAs followed by time-resolved electronics providing measurements of the energy spectra and their time variation. NPAs are calibrated using H/D atom beams of known energy and intensity. In the last decade solid-state detectors, and in particular natural diamond detectors (NDDs), were introduced for detection and energy analysis of the neutral particle fluxes from plasmas.

A superimposed E||B concept in which the electric field region was spatially displaced to follow the magnetic field region (i.e., tandem E||B) was developed in PPPL. The tandem E||B NPA enables simultaneous measurement of multiple mass species (e.g. H, D, and T or ^{3}He). Similar instruments have been developed for JT-60 and JET.

There are two important tasks for CX neutral particle diagnostics in ITER. The first task is the measurement of the hydrogen isotope composition of the plasma on the basis of measurements of neutralized fluxes of corresponding hydrogen ions, namely, protons, deuterons, and tritons in the 10- to 200-keV energy range. One of the main tasks of the ITER control system is to provide an optimal D-T ratio in the plasma. The second task of neutral particle diagnostics is the measurement of the distribution functions of MeV ions generated by auxiliary heating and fusion reactions. This includes measurement of the confined D-T α-particle distribution function by detection of He atom energy spectra in MeV range.

Figure 7 presents a tandem arrangement of two NPAs, which is proposed to be used on ITER. The NPA system consists of two devices: a low-energy NPA (LENPA) for the 10 to 200 keV energy range for providing measurement control of the isotope ratio and a high-energy NPA (HENPA) for the energy range 0.1 to 4 MeV to measure the fast ion and confined α-particle distribution functions by detection of the energy spectra of the neutralized fast ions and α-particles. Both the HENPA and the LENPA view along a major radius close to the equatorial plane of the torus and through the same straight vacuum opening of 20-cm diameter at the blanket face in the ITER port. Both analyzers can operate simultaneously because the LENPA is shifted horizontally to ensure an independent line of sight. Analyzers were successfully tested and used on JET.

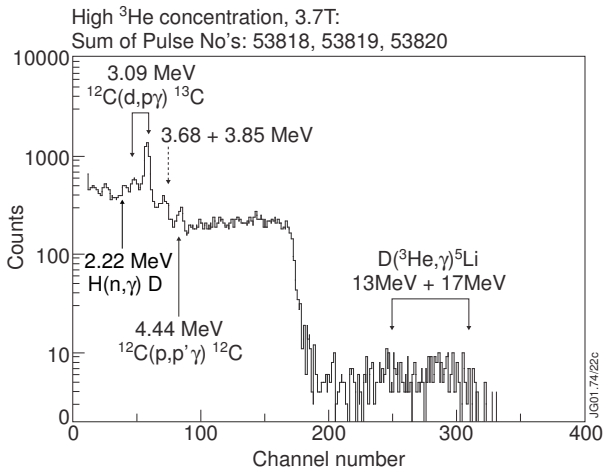

Fig. 8. Sum of gamma-ray energy spectra measured during three 2MA/3.7T discharges with ICRF heating tuned to $\omega=\omega_{c3He}$ in deuterium JET plasma with high ^3He concentration, $\eta_{He} \cong 20\%$.[14]

IV. GAMMA-RAY DIAGNOSTICS

One of the most important techniques used for studying fast-ion behaviours in fusion devices is nuclear reaction γ-ray diagnostics [13]. Measurements on the tokamaks Doublet-III, TFTR, JT-60U and JET have shown that an intense γ-ray emission is produced when fast ions (fusion products, ICRF-driven ions and NBI-injected ions) react either with plasma fuel ions or with the plasma impurities such as beryllium, boron, carbon and oxygen. On JET, the γ-ray emission measurements are routinely used to interpret different fast ion physics effects arising during ICRF and NBI heating.

There are three sources of fast particles that can give rise to a γ-ray emission from plasmas. Firstly, fusion reactions between the plasma fuel ions produce fusion products such as fast tritons, protons, ^{3}He and ^{4}He ions with MeV-energies. Secondly, ICRF heating of H- and ^{3}He-minority ions accelerates these ions to energies in the MeV range. There are also ICRF schemes to accelerate D, T and ^{4}He ions. Thirdly, NBI heating introduces D, T, H, ^{4}He and/or ^{3}He ions. Fast ions born in plasma produce line spectra due to their nuclear reactions with low-Z plasma

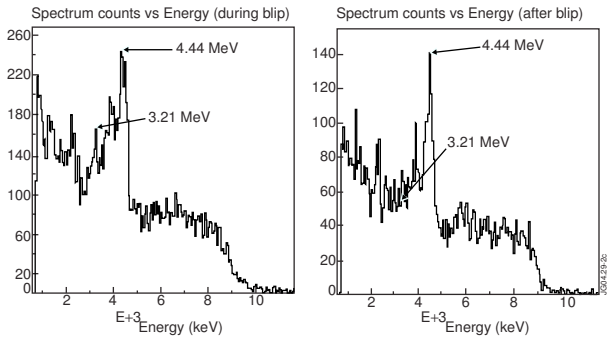

Fig. 9. Gamma-ray spectra measured in JET discharge with deuterium NBI heating and tritium 300-ms blip [16].

impurities. The fusion product neutrons interact with the structural materials, generating a continuous γ-ray background. A typical γ-ray spectrum recorded during ICRF heating with ^{3}He-ions shown in Fig.8. The 17-MeV γ-rays from the D(^{3}He, γ) ^{5}Li reaction, which used in JET as an indicator of the ICRF power deposition efficiency, were observed.

More than 15 essential nuclear reactions have been identified in the γ-ray spectra recorded at JET. Particularly, the reaction ^{9}Be(α,nγ)^{12}C, the significance of which was investigated in detail in Ref.15 for the fusion-born α-particle measurements. This is type of resonant reaction, which has thresholds. The presence of the 4.44-MeV peak in the γ-ray spectra is evidence for the existence of alphas with energies that exceed 1.7 MeV. The 3.21-MeV γ-rays indicate that the alphas with energies in excess of 4 MeV exist in the plasma. As an example, Fig.9 shows two γ-ray spectra, recorded in the same JET discharge: the left hand side plot shows the spectrum during 300-ms T-beam blip, the right one shows the spectrum just after the NBI blip. During the injection two γ-ray peaks, 4.44 MeV and 3.21 MeV are observed, however, in the post-blip time-slice the 3.21-MeV peak becomes rather weak. This is an effect of changes in the distribution function, i.e. the result of a shift of the high-energy tail to the low-energy range due to the α-particle slowing-down.

IV.A. Gamma-ray spectrometers in JET

In JET γ-ray energy spectra are measured with two different devices, one with a horizontal and one with a vertical line of sight through the plasma centre [14]. The first spectrometer is a calibrated bismuth germinate, $Bi_4Ge_3O_{12}$ (BGO) scintillation detector that is located in a well-shielded bunker and views the plasma tangentially. In order to reduce the neutron flux and the γ-ray background, the front collimator is filled with polythene. Behind the scintillation detector there is an additional dump of polythene and lead. The γ-rays are continuously recorded in all JET discharges over the energy range 1-28 MeV, with an energy resolution of about 4% at 10 MeV. The second device for the γ-ray energy spectrum measurements is a NaI(Tl) scintillation detector viewing the plasma vertically through the centre.

IV.B. Gamma-ray emission profile measurements

Spatial profiles of the γ-ray emission in the energy range E_γ>1 MeV have been measured in JET using the Gamma Cameras, which have ten horizontal and nine vertical collimated lines of sight. Each collimator defines poloidal-viewing extent at the centre of plasma of about 10 cm (Fig.3). The detector array is comprised of 19 CsI(Tl) photo-diodes (10 mm × 10 mm × 15 mm). Although the system was developed for neutron measurements and the shielding is not entirely adequate for γ-ray measurements, in discharges with ICRF heating the γ-ray measurements are successful.

In the Gamma Cameras the line-integral γ-ray brightness along the viewing direction is measured. Experimental data obtained for the 19 lines of sight are tomographically reconstructed to get the local γ-ray emissivity in a poloidal cross-section. In these reconstructions the full geometry of the collimators and detector efficiencies were taken into account, but small effects of attenuation and scattering of the γ-rays were neglected. It is assumed that the distribution of the low-Z impurities is uniform in the plasma core as confirmed by atomic spectroscopy measurements. For the tomographic reconstruction a constrained optimisation method [7] is used, which was successfully applied earlier to soft x-ray, bolometer and neutron measurements at JET. The effective spatial resolution of the diagnostic in these experiments is about 7cm.

The today data acquisition system accommodates the γ-ray count-rate measurement in four energy windows. This allows allocating specific γ-ray peaks in the windows to be counted separately. A typical example of the tomographic reconstruction of the measured line-integrated profiles is shown in Fig.10. It is seen clearly that the γ-ray emission profile produced by fast D-ions (right-hand figure) differs from the profile from ^{4}He-ions (left-hand figure) accelerated by ICRF [17]. This effect can be explained by the difference in pitch-angle distribution between ^{4}He beam-ions injected into the plasma quasi-tangentially and isotropic D-minority ions.

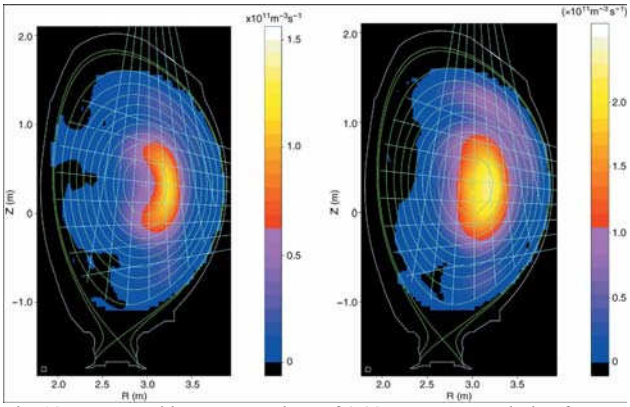

Fig. 10. Tomographic reconstructions of 4.44-MeV γ-ray emission from the reaction ^{9}Be(α,nγ)^{12}C (left) and 3.09-MeV γ-ray emission from the reaction ^{12}C(d,pγ)^{13}C (right) deduced from simultaneously measured profiles [17].

IV.C. Gamma-ray measurements in ITER

The gamma-ray diagnostics based on D(T,γ) ^{5}He and ^{9}Be(α,nγ)^{12}C reactions could provide important information on behaviour of the fusion alpha particles in ITER, where Be impurity is supplied from the first wall. The main idea of the technique consists of a comparison of both the 3.5-MeV alpha-particle birth profile (17-MeV γ-rays) and that of the confined α-particles slowed down to 1.7 MeV (4.4-MeV γ-rays). These measurements could be performed with a dedicated γ-ray profile camera, which is similar to the neutron/gamma camera currently in operation on JET. For time-resolved profile measurements, efficient γ-ray spectrometers and neutron attenuators, in each channel of the cameras, are needed.

General requirements of the spectrometers are high efficiency and peak-to-background ratio. It could be a single crystal spectrometer with heavy scintillator or a detector-array, which allow measurement of γ-rays in the energy range from 1 to 30MeV. The feasibility of the measurements also depends on the quality of neutron suppression of the collimators. A more convenient neutron filter is based on ^{6}LiH. It is compact, effective, and transparent for γ-rays and does not produce interfering γ-rays in the high energy range. A 30-cm sample of

the ^{6}LiH filter reduces 2.4-MeV neutron flux to ~900 times and the 15-MeV neutron flux to ~30 times.

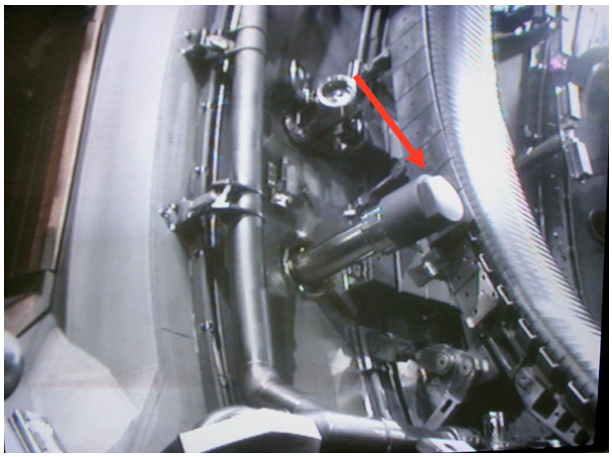

Fig.11. The scintillation probe installed in JET vessel.

The performance characteristics of the neutron ^{6}LiH attenuator were comprehensively investigated during experiments on JET [18]. The attenuator was used with collimated BGO spectrometer. The detector was placed in the laboratory above the tokamak and separated from it by a high-density concrete shielding 2-m thick. Analysis of the spectra (recorded with and without the ^{6}LiH attenuator) showed that without the attenuator γ-rays produced in reactions of the inelastic fast-neutron scattering by the detector material made the main contribution to the background counting rate of the detector. In the spectra measured with the ^{6}LiH attenuator, the background peaks are highly suppressed.

Gamma-ray cameras with such neutron filters seem to be the best candidates for measuring γ-ray spectra in the presence of high neutron fluxes typical of D-T reactor plasmas. The γ-ray cameras could be integrated with radiation shields of radial and vertical neutron cameras and have the same type of fan-shaped viewing geometry. Gamma-ray spectrometry induced by α-particles from beryllium tiles on the first wall using ^{9}Be(α,nγ)^{12}C reaction was proposed to measure the lost α-particle strength [19].

IV. MEASUREMENT OF FAST ION LOSSES

Fast ions, such as heating ions and α-particles, should be well confined until they transfer their energy to the plasma. In particular, α-particle heating will be needed to sustain ignition in fusion reactor plasma. Fundamental confinement properties can be studied by measurement of the α-particles loss. From the view point of machine protection, it is important to monitor the bombardment location and the heat load on the first wall. A clear understanding of loss mechanism is required to carry the fusion program to a real reactor. The temporal behaviour of lost alpha signals, and measurement of pitch angle and energy distribution are very important to understand the underlying physics, such as first orbit loss, toroidal field ripple loss, ICRH-induced loss and MHD induced loss.

In large tokamaks, like JET, a substantial part of the fusion-produced fast ions are confined. Dedicated probes were developed, and classical confinement properties, MHD induced losses, ripple effects, etc., are studied. For example, the alpha-particle loss measured by a scintillation probe [20] located at the TFTR vessel bottom showed dependence of loss ratios on the plasma current in the ion grad-*B* drift direction [21].

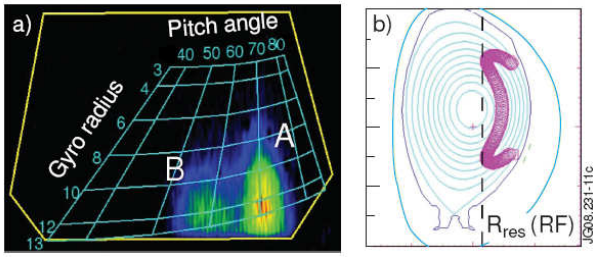

Fig.12. a) 2-D footprint of fast ion losses: fusion alphas from D^{3}He-reaction (A) and first orbit losses of p&T-fusion products from DD-reaction (B) observed on the scintillator plate; b) an orbit reconstruction for detected losses of type A [23].

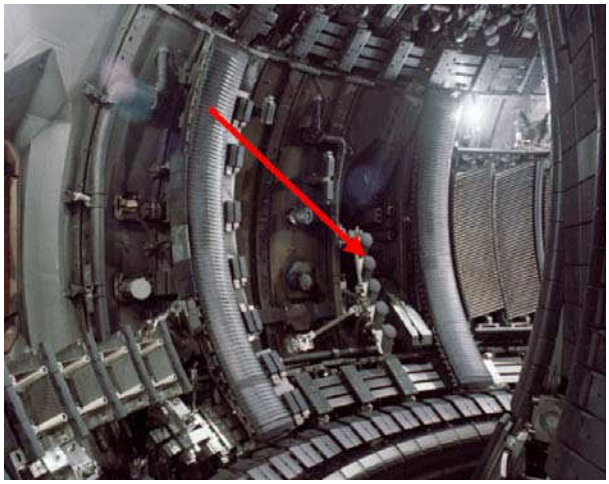

Fig.13. The Faraday Cup array installed in JET vessel.

Figure 11 shows the JET scintillator probe [22] in the vessel. Light emitted from the scintillator is divided by a beam splitter into two detection paths and is detected by the PMT array and charge-coupled device (CCD) camera. The PMT signals have high time resolution up to 1 kHz. The 2-D image obtained with the CCD camera provides information on both gyro-radius and pitch-angle simultaneously (Fig.12). As these probes are capable of resolving the energy and pitch angles of escaping fast ions with good time resolution, there is a great possibility of study of the MHD-induced losses.

In addition to SP the newly installed Faraday Cup array [24] could detect lost fusion alphas at multiple poloidal locations (Fig.13). The array consists of nine detectors spread over five poloidal locations below the mid-plane just outside the plasma at low magnetic field side of the JET torus. Along the major radius, the detectors are equally spaced in three locations. A detection of the temporal evolution of the fast α-particle current signals in the radially and poloidally distributed detectors can

provide a map of lost particle fluxes at different locations with time resolution of about 1 ms.

The Faraday Cups is the main measurement tools for time-resolved pitch angle and energy measurement of lost alphas in ITER. The self-heating of a D-T plasma by fusion-produced α-particles is the key to the realization of self-sustainable ignition of a thermonuclear plasma for fusion reactors. The loss of the α-particles means a deterioration of the heating input power. Moreover, the localization of alpha-particle bombardment on the first wall surface may induce serious damage. This is one of the key problems in ITER.

V. SUMMARY

Fusion product measurements, measurements of neutrons, γ-rays, and escaping MeV-ions produced in D-D, D-T, and other nuclear reactions are commonly used for diagnosing fusion plasmas magnetically confined. In D-D experiments on present devices, fusion reaction between a thermal and a non-thermal ion and that between non-thermal ions contribute substantially to the fusion reaction rate. Many interesting studies on energetic ion behaviours have been done by fusion product diagnostics. The recent publication on that issue can be found in [25 - 32]. For D-T fusion experiments on ITER, where the neutron emission rate will increase by more than of 10^3 from present large tokamaks and the thermonuclear fraction will be boosted as the self-heating source from α-particles becomes dominant, the fusion product diagnostics will be more important and will play the essential role, not only on the measurement of the fusion output power, but also on self-heating burning plasma studies.

ACKNOWLEDGMENTS

This work was funded jointly by the United Kingdom Engineering and Physical Sciences Research Council and by the European Communities under the contract of Association between EURATOM and UKAEA. This work was carried out within the framework of the European Fusion Development Agreement. The views and opinions expressed herein do not necessarily reflect those of the European Commission.

REFERENCES

1. M. SASAO, T. NISHITANI, J. KALLNE, V. KIPTILY, A. KRASILNIKOV and S. POPOVICHEV, “Chapter 9: Fusion product diagnostics”, *Fusion Sci. and Tech*., **53**, 604 (2008).
2. A. KISLYAKOV, A.J.H. DONNE, L.I. KRUPNIK, S.S. MEDLEY and M.P. PETROV, “Chapter 8: Particle diagnostics”, *Fusion Sci. and Tech*., **53**, 577 (2008).
3. V. G. KIPTILY, F. E. CECIL, and S. S. MEDLEY, *Plasma Phys. Control. Fusion*, **48**, R59 (2006).
4. H-B. BOSCH and G. M. JALE, *Nucl. Fusion*, 611 (1992).
5. O. N. JARVIS, *Plasma Phys. Control. Fusion* **36**, 209 (1994).
6. G. F. KNOLL, *Radiation Detectors*, John Wiley and Sons, New York (1979).
7. L.C. INGESSON et al *Nucl. Fusion* **38** 1675 (1998).
8. M. GATU et al., *Rev. Sci. Instrum.*, **77**, 10E702 (2006).
9. L. GIACOMELLI et al., *Nucl. Fusion*, **45**, 1191 (2005).
10. S. E. SHARAPOV et al., *Nucl. Fusion*, **40**, 1363 (2000).
11. R. K. FISHER et al., *Phys. Rev. Lett*., **75**, 846 (1995).
12. V. I. AFANASIEV et al., *Europhysics Conference Abstracts*. **27A**, O-4.4D (2003).
13. V. G. KIPTILY, F. E. CECIL, and S. S. MEDLEY, *Plasma Phys.Control. Fusion*, **48**, R59 (2006).
14. V. G. KIPTILY et al., *Nucl. Fusion*, **42**, 999 (2002).
15. V.G. Kiptily, *Fusion Technology,* **18,** 583 (1990).
16. V. G. KIPTILY et al., *Phys. Rev. Lett.*, **93**, 115001 (2004).
17. V. G. KIPTILY et al., *Nucl. Fusion*, **45**, L21 (2005).
18. I.N. CHUGUNOV et al., *Instrum. and Exp. Techniques*, **51**, 166 (2008).
19. V.G. KIPTILY et al., *Fusion Technology,* **22,** 454. (1992).
20. S.J. ZWEBEN, *Nucl. Fusion*, **29**, 825 (1989).
21. S.J.ZWEBEN et al., *Plasma Phys. Control. Fusion*, **39**, A275 (1997).
22. S. BAUMEL et al., Rev. Sci. Instrum. **75,** 3563 (2004).
23. V. KIPTILY et al., *Nucl. Fusion*, **49**, 065030 (2009).
24. D.S. DARROW et al., *Rev. Sci. Instrum*. **75,** 3566 (2004).
25. D.S. DARROW et al *Rev. Sci. Instrum.* **81**, 10D330 (2010).
26. V.G. KIPTILY et al, *Nuclear Fusion* **50** (2010) 084001.
27. M. TARDOCCHI et al *Phys Rev Letters* **107**, 205002 (2011)
28. T. GASSNER et al, *Phys. Plasmas* **19** (2012) 032115
29. M. NOCENTE et al, *Nucl. Fusion* **52** (2012) 063009
30. F.E. CECIL et al,, *Nucl. Fusion* **52** (2012) 094022
31. V.G. KIPTILY et al, *Plasma Phys. Control.Fusion* **54** (2012) 074010
32. V.G. KIPTILY et al, *Plasma and Fusion Research* **8** (2013) 2502071.